A Comparison of Core and Crosswell Seismic Data from a Carbonate Reservoir*

K.E. Tucker[1]. and P.M. Harris[2]

Search and Discovery Article #60047 (2009)
Posted June 4, 2009

*Reprint of Tucker, K.E., and P.M. Harris, 1998, A Comparison of Core and Crosswell Seismic Data from a Carbonate Reservoir: West Texas Geological Society Bulletin, v. 37 (9), p. 5-14. Appreciation is expressed to WTGS (http://www.wtgs.org/Home/tabid/36/Default.aspx) and to Paula Mitchell, Executive Director, for permission to post this article.

[1]Chevron Petroleum Technology Company, LaHabra, CA; currently Huntington Beach, CA (ktkr2@aol.com)
[2]Chevron Petroleum Technology Company, LaHabra, CA; currently ETC, Chevron, San Ramon, CA, USA. (MitchHarris@chevron.com)

Abstract and Contents

Abstract

By making detailed comparisons with core data from a well located on a crosswell seismic profile, we examine the vertical resolution of crosswell seismic data from a geologic perspective. Whole-core porosity and permeability measurements are highly variable in our example and are not obviously related to core-based lithofacies. The disconnect between reservoir quality and depositional lithofacies is caused by a complex diagenetic overprint, primarily cementation by evaporites. Changes in porosity and mineralogy (predominantly gypsum and siliciclastic abundance) relate directly to the numerous crosswell seismic events. Although major stratigraphic boundaries (sequence boundaries and flooding surfaces) generally coincide with reflectors, lithofacies and small-scale depositional cycles recognized during the core description do not relate directly to the seismic data. There are strong indications that crosswell seismic data can be an important tool for assessing reservoir variability.

Contents

Reprinted with permission of the Canadian Society of Petroleum Geologist from the following publication: Wood, J. and Martindale, B. (eds.), Sedimentary Events and Hydrocarbon Systems: 1997 CSPG/SEPM Joint Convention Core Conference, p. 223-236.

A Comparison of Core and Crosswell Seismic Data from a Carbonate Reservoir

TUCKER, KARLA E., and PAUL M. HARRIS, Chevron Petroleum Technology Company, La Habra, CA

Abstract

By making detailed comparisons with core data from a well located on a crosswell seismic profile, we examine the vertical resolution of crosswell seismic data from a geologic perspective. Whole-core porosity and permeability measurements are highly variable in our example and are not obviously related to core-based lithofacies. The disconnect between reservoir quality and depositional lithofacies is caused by a complex diagenetic overprint, primarily cementation by evaporites. Changes in porosity and mineralogy (predominantly gypsum and siliciclastic abundance) relate directly to the numerous crosswell seismic events. Although major stratigraphic boundaries (sequence boundaries and flooding surfaces) generally coincide with reflectors, lithofacies and small-scale depositional cycles recognized during the core description do not relate directly to the seismic data. There are strong indications that crosswell seismic data can be an important tool for assessing reservoir variability.

Introduction

A joint Stanford University-Industry project, associated with a CO_2 flood pilot being conducted in the McElroy Field of west Texas (Fig. 1), has demonstrated that very high resolution reflection images can be obtained in carbonate reservoirs using crosswell seismology (Harris et al., 1995). In this study we examine the vertical resolution of crosswell seismic data from a geologic perspective by making detailed comparisons with core data from a well located on one end of a crosswell profile. McElroy Field is a very mature field; i.e., close well spacing and advanced types of reservoir processing are either already in place or being planned. We feel that there are strong indications that crosswell seismic data can be an important tool for assessing reservoir variability vertically and between well locations in the field. Therefore, it is likely that crosswell seismic will play an increasingly important part in reservoir characterization of McElroy and other fields like it.

The main reservoir in McElroy Field occurs within the Grayburg Formation (Permian, Lower Guadalupian), and the main pay interval has an approximately 80-ft (24 m) gross reservoir thickness. A broad spectrum of deposits, ranging from shoreline and inner ramp on the west to deeper-water outer-ramp environments toward the east, accumulated along the eastern margin of the Central Basin Platform bordering the Midland Basin (Fig. 1). The depositional slope across the portion of the shelf that now comprises the field was gradual, possibly interrupted only by localized bars of carbonate sand or small reefs. Core studies show the Grayburg carbonate shelf deposits in McElroy Field to be anhydritic dolostones that become increasingly evaporitic and silty toward the top of the Grayburg Formation and into the overlying Queen Formation. Terrigenous sediments and evaporites of the lower Queen Formation provide a cap and seal for the Grayburg reservoir rocks. The overall depositional succession within the Grayburg is a series of upward-shallowing and generally eastwardly prograding carbonate units (Fig. 2). The lower Grayburg represents more open ramp environments, the middle Grayburg reservoir zone represents shallower ramp environments, and the upper Grayburg represents nearly intertidal environments. The basal contact of the Grayburg is a pronounced unconformity with the underlying San Andres Formation, whereas the top contact with the Queen Formation is a more subtle unconformity.

Conventional Core Description

Conventional core was taken from 2775 to 3060 ft core depth (2779-3064 ft log depth) in the 1202 well as part of the crosswell seismic project. The core from the well is divided into major depositional units (Fig. 3) that are part of a sequence stratigraphic framework developed for the field (Lindsay, 1995, pers. comm.). The bottom 20 ft (6 m) of core (core depth = 3040-3060 ft) consists principally of ooid and peloid dolopackstones/grainstones that are organized within several upward-shallowing depositional cycles. Evidence for subaerial exposure marks the top of some of the cycles. A more pronounced interval with evidence for subaerial exposure - i.e., teepee structures, breccias, and conglomerates - is picked as the unconformable sequence boundary separating the San Andres and Grayburg formations (3040 ft core depth; 3044 ft log depth).

Immediately above the formation boundary is a 21-ft (6.4 m) thick interval (core depth = 3019-3040 ft) containing a thin dolomitic sandstone, overlain by predominately ooid, but some peloid, dolopackstone/grainstones that are contained within three depositional cycles (Fig. 3). Field-wide stratigraphic studies by Lindsay (1995) show that this interval

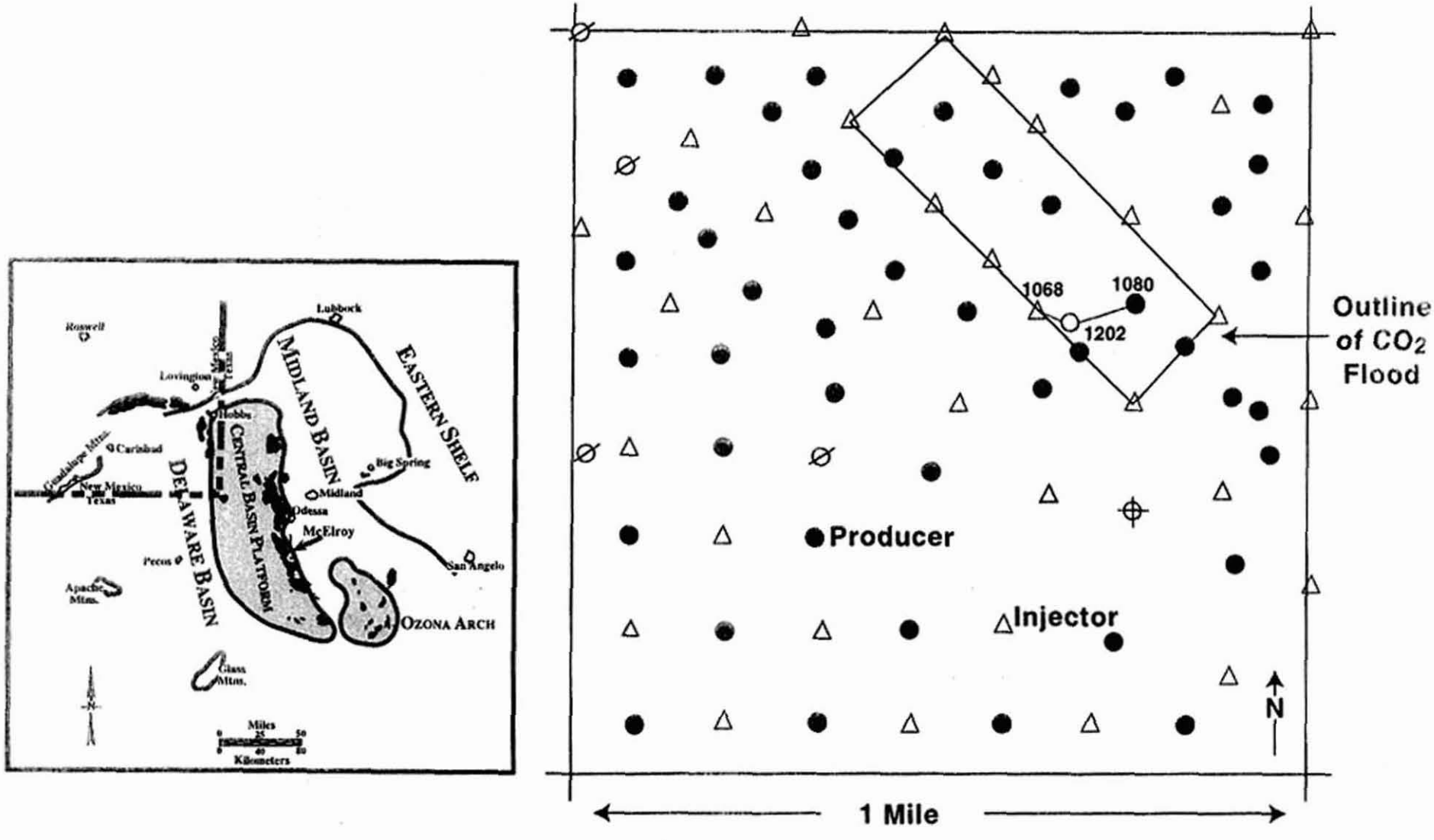

Figure 1. The CO_2–flood pilot area is in the northeast quadrant of Section 205 of McElroy Field, which itself is on the eastern edge of the Central Basin Platform (see inset: a general geology map of west Texas). Two crosswell seismic profiles were acquired between wells 1068 and 1202 (profile 1 which is emphasized in this study) and wells 1202 and 1080 (profile 2).

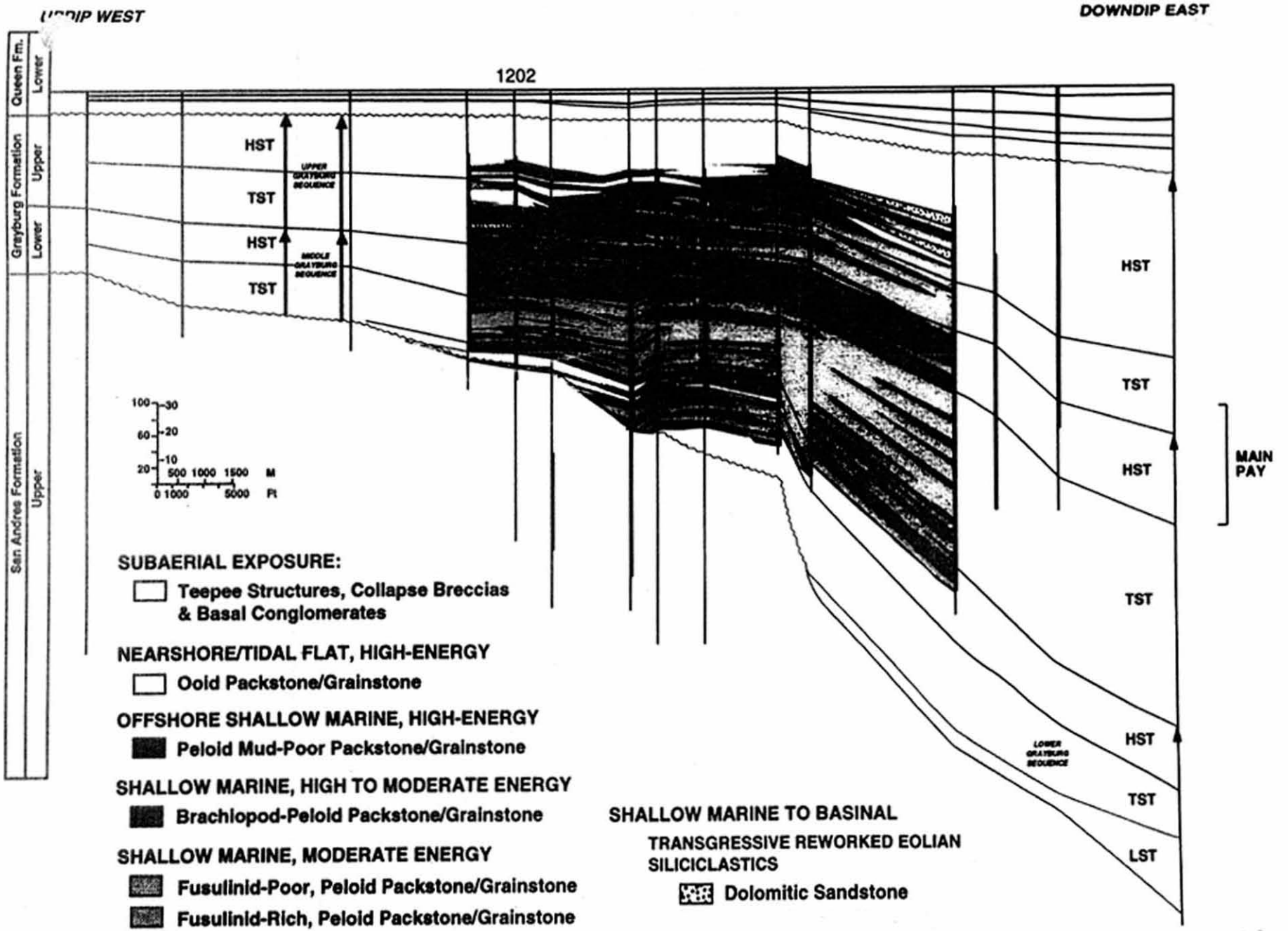

Figure 2. McElroy Field sequence stratigraphic framework (modified from Lindsay, 1995) showing location of the 1202 well. Significant vertical and horizontal facies changes occur across the field. Vertical lines are well control; thicker bars are cored intervals. See Figure 3 for definition of LST, TST, and HST; as well as details of the 1202 core.

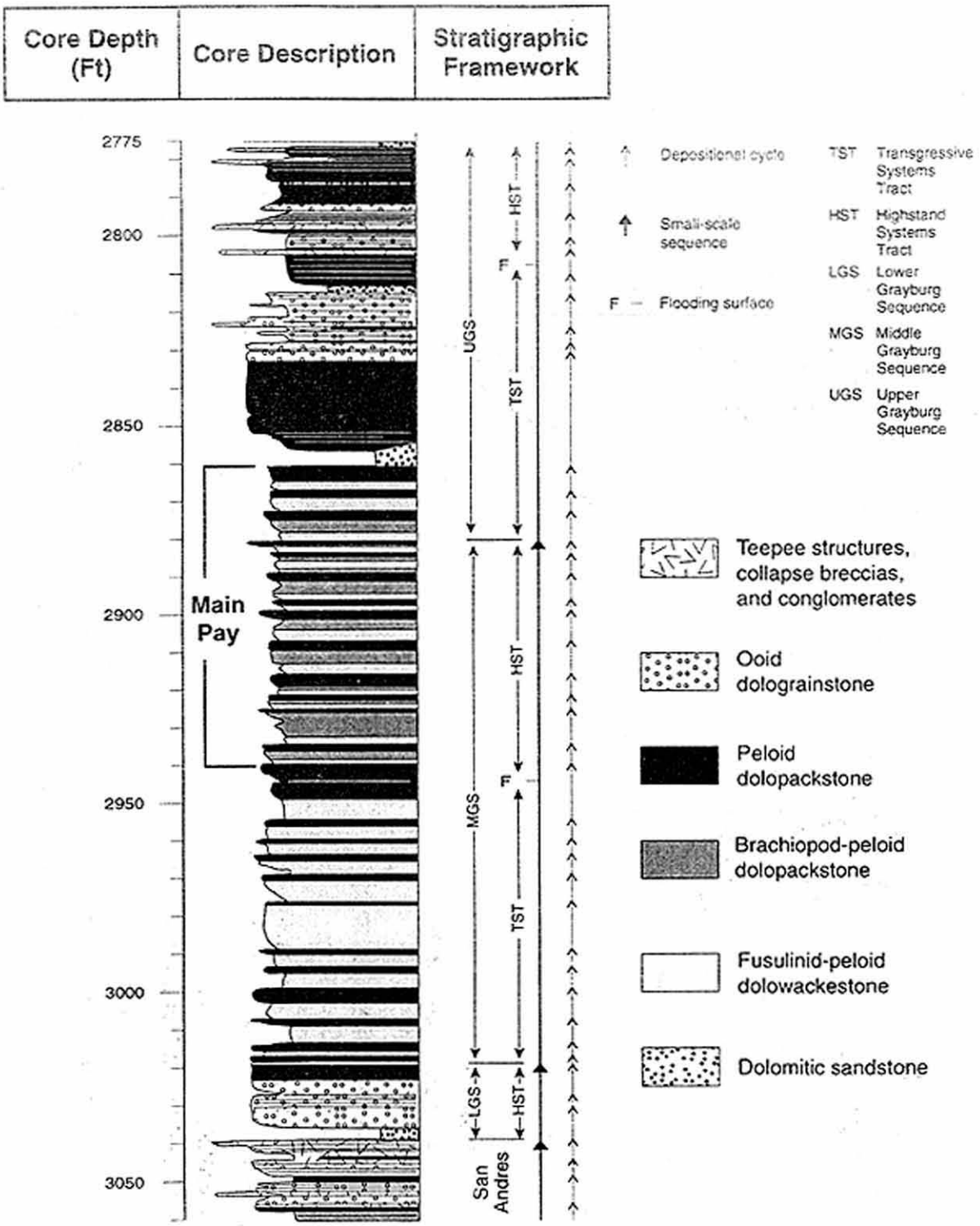

Figure 3. Core description from the 1202 well (modified from Lindsay, 1995, and personal communication). Major lithofacies (grain types and depositional texture) and sequence stratigraphic units are compared with crosswell and other data on subsequent figures.

thickens substantially to the east and is the lowermost of three small-scale sequences recognized within the Grayburg (Fig. 2). Only the uppermost highstand systems tract portion of this lowermost Grayburg sequence occurs in the 1202 well. The onlap of the underlying transgressive systems tract terminates further to the east.

The remainder of the 1202 core contains varied lithologies that comprise the middle and upper Grayburg sequences recognized by Lindsay (1995). The middle sequence contains a transgressive system tract 74 ft (22.5 m) thick (core depth = 2945-3019 ft) of predominately dolopackstone/grainstone rich in fusulinid benthic foraminifers and peloids (Fig. 3). Depositional cycles are delineated where the packstone/grainstones become more peloid-rich, a probable indicator of slight shallowing. Above a maximum flooding surface, the middle Grayburg highstand systems tract (core depth = 2880-2945 ft) contains predominately brachiopod and peloid packstone/grainstones and lesser amounts of the fusulinid packstone/grainstone, and probably represents a shallower-water and higher-energy depositional setting than the fusulinid section below. Numerous depositional cycles can be differentiated based on the general fusulinid-, brachiopod-, and peloid-rich succession. This highstand, 65-ft (19.8 m) thick portion (core depth = 2880-2945 ft) of the core, along with the overlying 19 ft (5.8 m) (core depth = 2861-2880 ft), corresponds to the main pay interval in this part of the field (Fig. 2).

The upper Grayburg sequence was not completely cored in the 1202 well and, as a result, is more difficult to characterize. The field-wide studies of Lindsay (1995) show this sequence to be more completely developed in a downdip direction to the east of the well (Fig. 2). The transgressive systems tract, 72 ft (22 m) thick in the core (core depth = 2808-2880 ft), is predominately peloid packstone/grainstones, with some ooid packstone/grainstones in the upper part and minor fusulinid-rich packstone/grainstone in the lower portion (Fig. 3). Depositional cycles are picked by fusulinid-peloid variations in the lower part, peloid-ooid variations in the middle, and evidence for minor subaerial exposure in the upper ooid-rich part. Only the lower 33 ft (10 m) (core depth = 2775-2808 ft) of the highstand systems tract of the upper sequence is cored in the 1202 well, which extends upward another 60 ft (18 m), as shown by log correlations with other wells (Fig. 2). The core contains alternating peloid and ooid packstone/grainstones, which is the basis for picking depositional cycles. Evidence from other wells shows that the upper portion of the highstand systems tract becomes more ooid-rich, contains numerous siliciclastic beds, and is generally of a much shallower water character.

Whole-Core Analysis

Routine whole-core analysis (285 samples) was completed on 6-in. (15 cm) lengths of full-diameter core from almost every foot along the entire length of the 1202 core (Harris et al., 1995; Nolen-Hoeksema et al., 1995; Fig. 4). In addition, permeability was measured using a minipermeameter at 6-in. (15 cm) sample spacing along the full length of core. These data provide petrophysical and mineralogical information that, in combination with the core description, are necessary to interpret the crosswell data.

The whole-core samples were cleaned using a low-temperature toluene-CO_2 extraction method. The low temperature (less than 104°F or 40°C) produced minimal dehydration of the gypsum ($CaSO_4 \cdot 2H_2O$) in the rock (Hurd and Fitch, 1959). Fluid saturations were determined from the fluids collected during the core cleaning process. After each sample was cleaned and dried, the porosity, permeability, and grain density were determined. This first porosity measurement is referred to as the "low-temperature porosity" (LTPor). The core samples were then heated to a high temperature to drive off the water of hydration in the gypsum. After cooling, the "high-temperature porosity" (HTPor) was measured. Gypsum content was calculated from the weight loss and increase in porosity, i.e., pore volume, that resulted from reheating the sample (Hurd and Fitch, 1959). This assumes that both effects are the result of the alteration of gypsum to anhydrite ($CaSO_4$) by dehydration, which causes a decrease in grain volume.

For the 285 full-diameter core samples, the LTPor ranged from 0.5% to 20.9% and averaged (arithmetic mean) 7.4%, whereas the HTPor ranged from 0.8% to 21.1% and averaged 9.7%. Steady-state permeability to air ranged from less than 0.01 md to 217 md and averaged (geometric mean) 0.6 md. As expected, LTPor, permeability, and oil saturation are higher overall in the main pay interval (average 12%, 5 md, and 32% respectively); however, isolated zones above and below the main pay interval also have good reservoir characteristics. The highly variable nature of porosity and, to a greater degree, permeability are evident in Figure 4.

Variable amounts (0-25%) of gypsum are present throughout the core, although gypsum abundance does not appear to be lithofacies-specific based on whole-core measurements. Two general observations can be made regarding the stratigraphic distribution of gypsum. First, the highest frequency variations in gypsum content occur within the middle and lower Grayburg sequences (2885-3044 ft), which have the best reservoir quality. Second, the greatest volumes of gypsum cement occur almost immediately above the siliciclastic beds at 2861 and 3041 ft (Fig. 4).

Figure 5 shows crossplots of whole-core data by lithofacies. The peloid dolopackstone, brachiopod-peloid dolopackstone, and fusulinid-peloid dolowackestone are the primary reservoir lithofacies, whereas the dolomitic sandstone, ooid dolograinstone, and teepee lithofacies are mostly nonreservoir. Figure 5A shows a good correlation between porosity and permeability, except for a group of samples on the left that may be fractured. Figure 5B and C shows porosity plot-

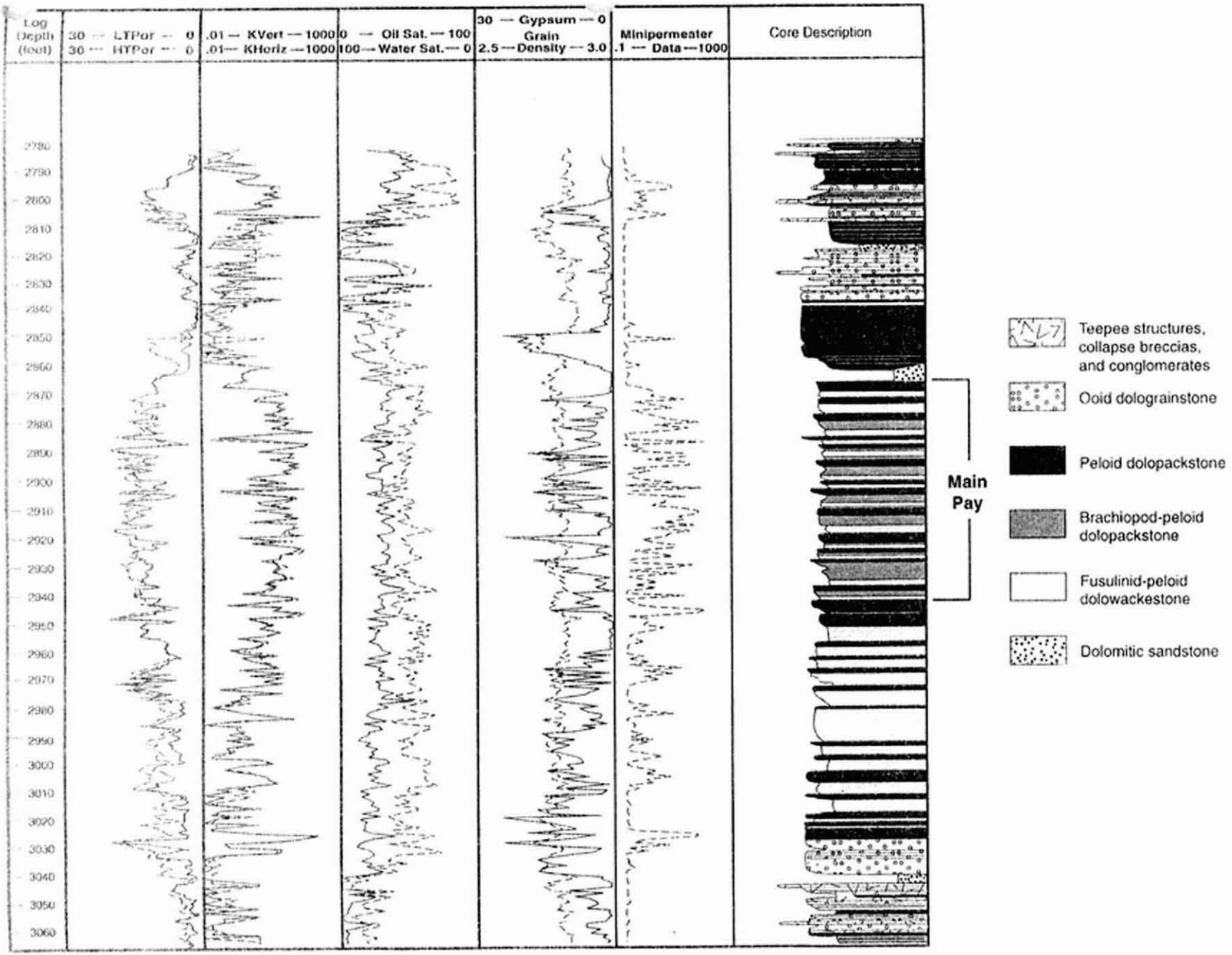

Figure 4. Whole-core analysis (285 samples) and minipermeameter data plotted vs depth for the 1202 well and compared with the core description provide petrophysical and mineralogical information that are needed to interpret the crosswell seismic data.

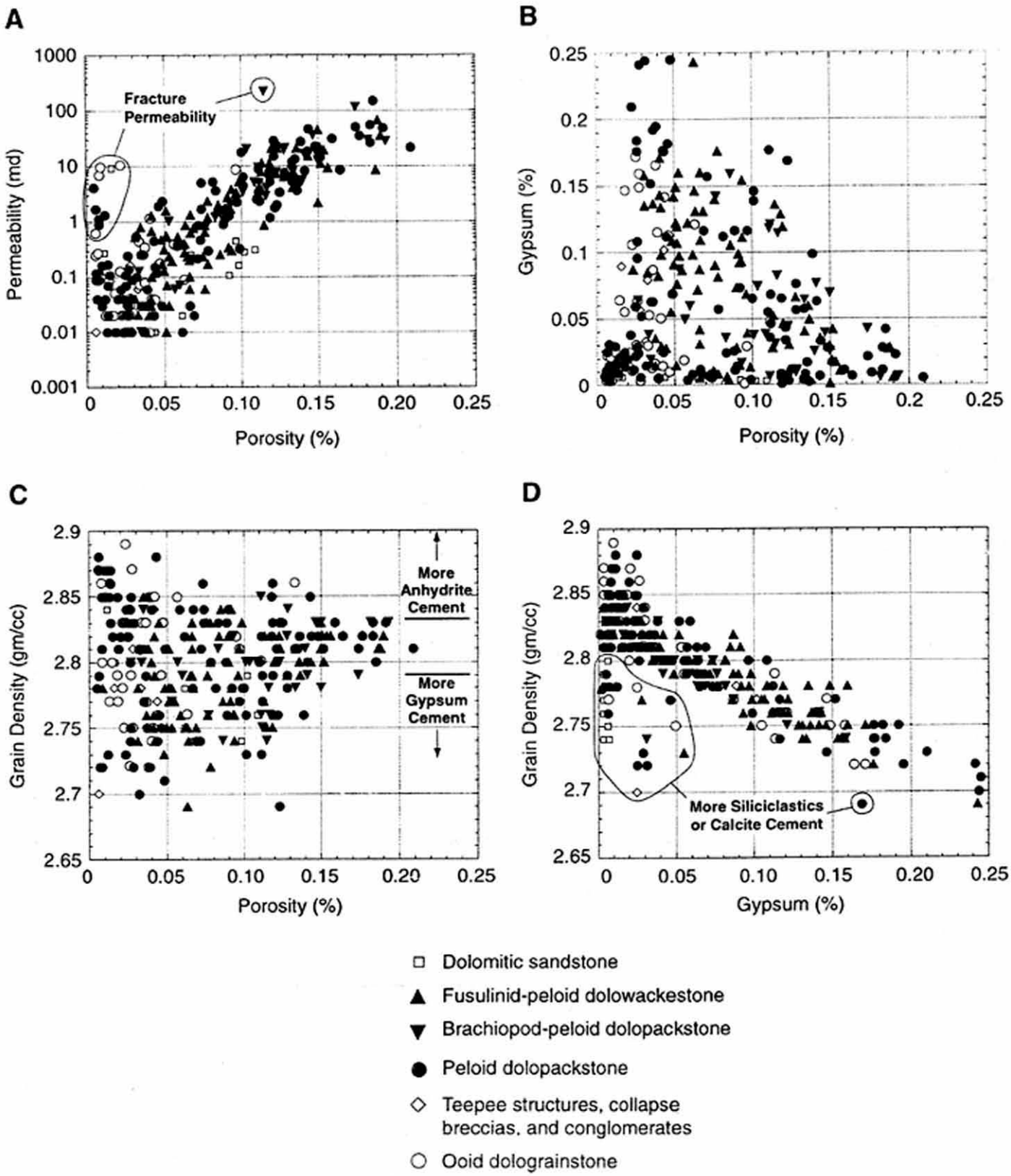

Figure 5. Crossplots of (A) permeability, (B) gypsum content, and (C) grain density vs porosity (low temperature), and (D) grain density vs gypsum content for all whole-core data. All crossplots are coded according to lithofacies from the core description of Figure 3. Permeability data have an imposed minimum of 0.01 md, which was the lower limit of the permeameter. Gypsum content was calculated from the difference between high- and low- temperature porosity measurements following Hurd and Fitch (1959).

ted against gypsum and grain density respectively, to illustrate the complicated diagenetic overprint present in McElroy samples. In particular, Figure 5B shows there is little-to-no systematic relation between gypsum content and porosity, except that the highest porosity samples uniformly contain ess than 5% gyp-sum. Figure 5C shows that there is a significant amount of anhydrite as well as gypsum reducing porosity; the highest porosity samples have uniform grain densities, which is consistent with the conclusion that porosity has been modified by post-depositional cementation. Figure 5D shows a very close correlation between grain density and gypsum content, except for samples that may be cemented with calcite or contain significant amounts of siliciclastic material. In fact, Figure 5B and D shows that the dolomitic sandstone samples uniformly have little or no gypsum cement, which suggests that the dolomitic sandstones may have been conduits for diagenetic fluids. Summarizing the important points: cementation by gypsum and anhydrite is ubiquitous and not lithofacies-specific; siliciclastics and calcite cement are present in a few samples in variable amounts.

Comparison Of Crosswell Seismic And Core Data

Crosswell seismic reflection images can be related to the stratigraphy, lithofacies, porosity, and mineralogy recognized in the 1202 core. Changes in porosity and mineralogy (predominantly gypsum and siliciclastic abundance) relate directly to the numerous seismic events. Although major stratigraphic boundaries (sequence boundaries and flooding surfaces) generally coincide with reflectors, lithofacies and small-scale depositional cycles recognized during the core description do not relate directly to the seismic data.

The apparent resolution in the P- and S-wave reflection images of Figure 6 is quite striking; the wavelengths are on the order of 9 to 13 ft (3-4 m). In contrast, traditional surface P-wave seismic data in the study area usually have an upper frequency limit on the order of 100 Hz, resulting in wavelengths of approximately 150 to 200 ft (45-60 m), assuming P-wave velocities of 15,000 to 20,000 ft/s. Therefore, the main pay interval in McElroy Field is less than one-third wavelength on the surface seismic data.

The main pay interval is from 2860 to 2940 ft on the P- and S-wave reflection images from profile 1 (Fig. 6). The P-wave image has about five continuous events within the 80-ft (24 m) main pay interval, whereas the S-wave image has about eight continuous events. Both images came from the same dataset (Harris et al., 1995), and the frequency content is about the same in both. Therefore, to some extent, the higher resolution of the S-wave image results because S-wave velocities are lower than P-wave velocities; hence S wavelengths are shorter than P wavelengths.

Most positive amplitude (filled) events in the reflection images seem to correlate with changes in porosity and mineralogy as described in the core and measured during core analysis. The positive amplitude, continuous reflections near the top of both the P- and S-wave images (2725-2775 ft; all depths are log depths) are related to the interbedded siliciclastic and carbonate beds straddling the Grayburg-Queen boundary (Fig. 6). The next interval, between 2775 ft and the top of the main pay, has few events because the interval is mostly tight and petrophysically fairly homogeneous. Positive S-wave reflections in this zone appear to be related to a decrease in porosity in the first high-porosity zone (~2800 ft), the base of two lower-porosity zones (~2825 and ~2835 ft), and the base of a gypsum-cemented, lower-porosity zone (~2854 ft) recognized in the core. Positive P-wave reflections coincide with the depths described above except for 2835 ft, which may be masked by the very high-amplitude, positive P-wave reflection at ~2842 ft. This reflector, which is not present on the S-wave image, coincides with the top of a gypsum-cemented interval.

The positive moderate to high amplitude, fairly continuous reflections within the main pay interval, which are coincident mostly with the highstand systems tract of the middle Grayburg sequence, are primarily related to the high degree of porosity and gypsum cement variation. For example, the first positive event on the S-wave image in the main pay interval coincides with the base of the first high gypsum streak and a porosity decrease (~2874 ft). The underlying positive event on the S-wave image corresponds to the top of a tight streak (~2883 ft) that coincides with the sequence boundary between the upper and middle Grayburg sequences. Similarly almost all of the S-wave positive events in the main pay interval correspond to decreases in porosity and/or gypsum (2888, 2896, 2902, 2912, 2922, 2929, and 2935 ft). Positive P-wave reflections coincide with many of the depths described above; however, some of the other positive S-wave reflections combine in groups of two into a single, positive P-wave reflection (e.g., S-wave at 2896 and 2902 ft = P-wave at 2900 ft).

The positive moderate to high amplitude, fairly continuous reflections between the base of the main pay and 3015 ft, which coincide with the mostly fusulinid-rich transgressive system tract of the middle Grayburg sequence, are also related to the high degree of porosity and gypsum variation. To illustrate this, the first positive event on the S-wave image below the main pay interval is coincident with the base of a gypsum-cemented zone (~2945 ft), which also corresponds to the maximum flooding surface that separates the more peloid-rich highstand system tract above from the more fusulinid-rich transgressive system tract below. Another positive event on the S-wave image coincides with a major porosity decrease (~2956 ft). As described for the interval immediately above, almost all of the positive events on the S-wave image in this interval correspond to decreases in porosity and/or gypsum. Similarly most of the positive P-wave reflections appear to represent groups of two S-wave reflections.

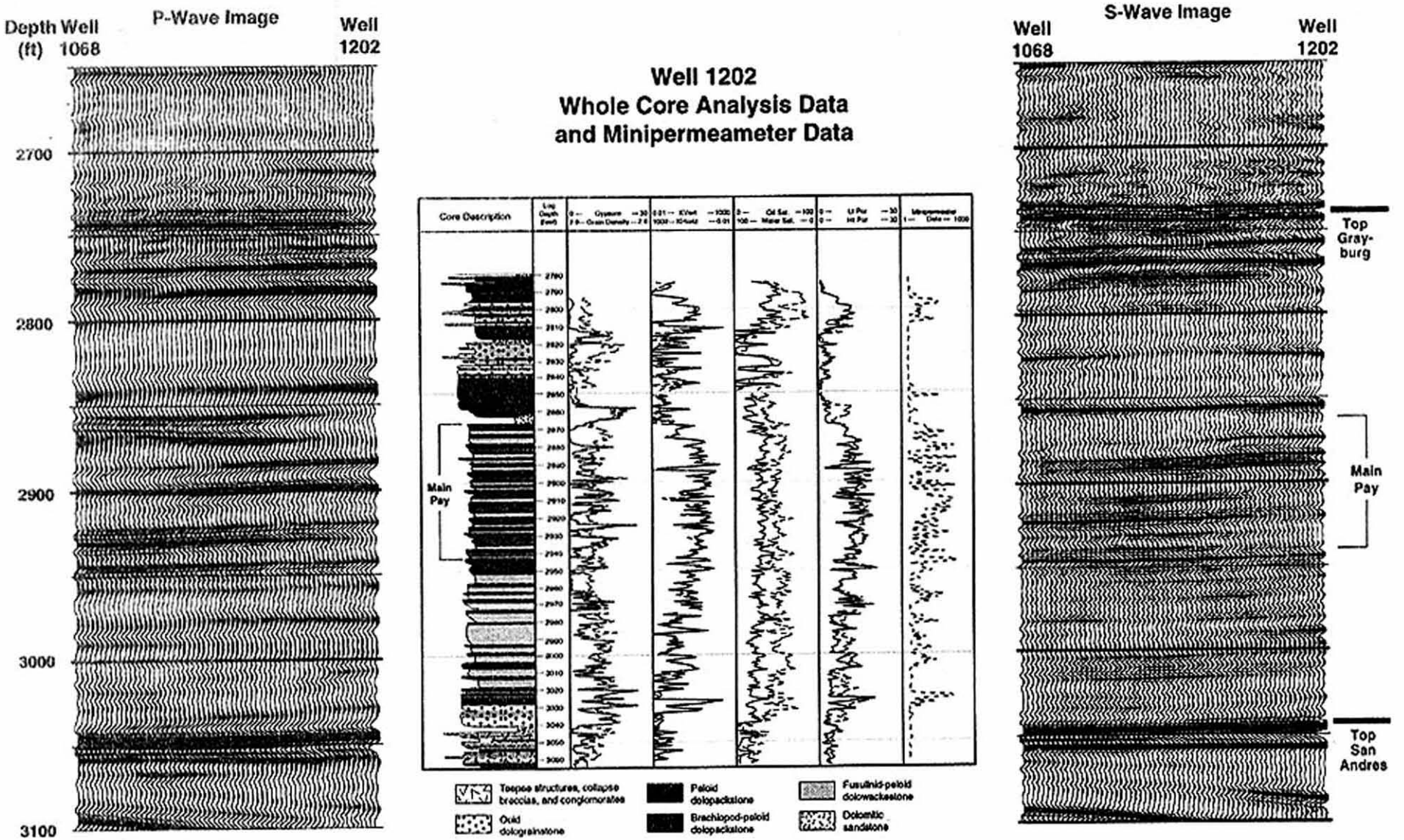

Figure 6. Whole-core analysis data, minipermeameter data, and core description for the 1202 well compared with the P-wave (left) and S-wave (right) crosswell seismic reflection images for profile 1. Most positive amplitude events on the crosswell data correlate with changes in porosity and/or mineralogy (mostly gypsum).

The positive, moderate amplitude, fairly continuous S-wave reflections from ~3015 ft to the San Andres/Grayburg contact are associated with the ooid and peloid dolopackstones/grainstones of the lowermost Grayburg sequence. These reflections are related to gypsum-cemented zones, the dolomitic sandstone bed, and porosity variations. For example, the first positive event on the S-wave image in this interval is related to the base of a high gypsum streak (~3022 ft) that also coincides with the sequence boundary between the lower and middle Grayburg sequences. Another positive event on the S-wave image is coincident with a decrease in porosity and gypsum cement (~3028 ft). The next positive event on the S-wave image coincides with the base of a gypsum-cemented zone and the top of the dolomitic sandstone bed (~3040 ft). Positive P-wave reflections are present for the first two depths described above. No reflection is apparent at 3040 ft, possibly because it is masked by the strong positive reflector at 3045 ft.

One very striking feature on the P- and S-wave images is the two prominent positive reflectors (3045 and 3060 ft) that coincide approximately with the sequence boundary between the Grayburg and San Andres formations at 3040 ft (Fig. 6). Although this sequence boundary is a pronounced unconformity and is quite clear in the reflection images, the boundary is often difficult to identify in core, logs, and 2-D surface seismic. The high-amplitude, continuous reflectors at the San Andres/Grayburg contact and the dipping reflectors almost immediately below correspond with the interbedded siliciclastic and dolostone beds of the upper San Andres.

Conclusions

By comparing changes observed and measured in the core from the 1202 well to crosswell seismic reflection images, we conclude that (1) total porosity has the strongest influence on velocity and acoustic impedance; therefore, changes in porosity are a primary cause of reflections; and (2) changes in mineralogy, including variations in the amount of evaporite cement and siliciclastics, also affect velocity and acoustic impedance. A significant result of the diagenetic complexity of the McElroy reservoir is that reservoir quality does not match original depositional facies, but is instead controlled by a complicated mixture of depositional and diagenetic effects. This is particularly true for the main pay interval and makes interpreting the crosswell images in terms of lithofacies, or the small-scale depositional cycles that they are grouped in, somewhat meaningless. However, since the crosswell images do appear to be responding to fine-scale variations in porosity, perhaps log-based stratigraphic units based on porosity are the most appropriate "flow unit" or "reservoir engineering" type of facies to be identified for reservoir characterization.

Based on our comparison of core and crosswell seismic data, we conclude that crosswell seismic is capable of high-resolution reservoir delineation, and its usefulness for reservoir analysis should continue to be investigated.

Acknowledgments

We acknowledge the help of many who made our work and publication possible: Richard C. Nolen-Hoeksema (University of Michigan) for collaboration on many aspects of our crosswell investigations; Bob Lindsay (Chevron U.S.A.) for data and valuable discussions on McElroy Field; Bob Langan (Chevron Petroleum Technology Company) and Jerry Harris (Stanford) for valuable technical discussions and vision; and Spyros Lazaratos (Tomoseis) for the reflection images at various stages of processing improvements. We especially thank Chevron Petroleum Technology Company for technical support and permission to publish.

References

Harris, J. M., Nolen-Hoeksema, R. C., Langan, R. T., Van Schaack, M., Lazaratos, S. K., and Rector, J. W., III, 1995, High resolution imaging of a west Texas carbonate reservoir: Part 1 - Project summary and interpretation: Geophysics, v. 60, no. 3, pp. 667-681.

Hurd, B. G. and Fitch, J. L., 1959, The effect of gypsum on core analysis results: Petroleum Transactions, AIME, v. 216, pp. 221-224.

Lindsay, R. F., 1995, Carbonate sequence stratigraphy on the development geology scale: outcrop and subsurface examples from the Permian Grayburg Formation, Permian Basin (abs.), *in* Pause, P. H. and Candelaria, M. P. (eds.), Carbonate Facies and Sequence Stratigraphy: Practical Applications of Carbonate Models: Permian Basin Section SEPM Publication 95-36, p. 205.

Nolen-Hoeksema, R. C., Wang, Z., Harris, J. M., and Langan, R. T., 1995, High resolution imaging of a west Texas carbonate reservoir: Part 5 - Core analysis: Geophysics, v. 60, no. 3, pp. 712-726.